



Published in final edited form as:

Biomaterials. 2014 January ; 35(2): 856–865.

The genotype-dependent influence of functionalized multiwalled carbon nanotubes on fetal development

Xinglu Huang^a, Fan Zhang^a, Xiaolian Sun^a, Ki Young Choi^a, Gang Niu^a, Guofeng Zhang^b, Jinxia Guo^a, Seulki Lee^a, and Xiaoyuan Chen^{a,*}

^aLaboratory of Molecular Imaging and Nanomedicine (LOMIN), National Institute of Biomedical Imaging and Bioengineering (NIBIB), National Institutes of Health (NIH), Bethesda, MD 20892, USA

^bBiomedical Engineering and Physical Science Shared Resource, National Institute of Biomedical Imaging and Bioengineering (NIBIB), National Institutes of Health (NIH), Bethesda, MD 20892, USA

Abstract

In many cases cancer is caused by gene deficiency that is being passed along from generation to generation. Soluble carbon nanotubes (CNTs) have shown promising applications in the diagnosis and therapy of cancer, however, the potential relationship between cancer-prone individuals and response to CNT exposure as a prerequisite for development of personalized nanomedicine, is still poorly understood. Here we report that intravenous injections of multi-walled carbon nanotubes into p53 (a well-known cancer susceptible gene) heterozygous pregnant mice can induce p53-dependent responses in fetal development. Larger sized multi-walled carbon nanotubes moved across the blood-placenta barrier (BPB), restricted the development of fetuses, and induced brain deformity, whereas single-walled and smaller sized multi-walled carbon nanotubes showed no or less fetotoxicity. A molecular mechanism study found that multi-walled carbon nanotubes directly triggered p53-dependent apoptosis and cell cycle arrest in response to DNA damage. Based on the molecular mechanism, we also incorporated N-acetylcysteine (NAC), a FDA approved antioxidant, to prevent CNTs induced nuclear DNA damage and reduce brain development abnormalities. Our findings suggest that CNTs might have genetic background-dependent toxic effect on the normal development of the embryo, and provide new insights into protection against nanoparticle-induced toxicity in potential clinical applications.

Keywords

Carbon nanotubes; nanotoxicity; genetic background; blood-placenta barrier; fetal development

To whom correspondence may be addressed. Shawn.Chen@nih.gov.

Publisher's Disclaimer: This is a PDF file of an unedited manuscript that has been accepted for publication. As a service to our customers we are providing this early version of the manuscript. The manuscript will undergo copyediting, typesetting, and review of the resulting proof before it is published in its final citable form. Please note that during the production process errors may be discovered which could affect the content, and all legal disclaimers that apply to the journal pertain.

1. Introduction

Carbon nanotubes (CNTs) have attracted increased attention since their discovery because of their unique physical and chemical properties [1]. However, information concerning the potential health hazards of CNTs remains inadequately explored. Previous reports have shown that, under certain inhalation exposures, CNTs either activate cyclooxygenase enzymes in the spleen to suppress systemic immune function [2] or induce subpleural fibrosis [3]. Although inhalation is the most relevant method for determining the toxicity of CNTs, more researchers pay attention to the acute and chronic toxicity of water-soluble, functionalized CNTs when the CNTs enter the bloodstream. This is so for a number of reasons: (i) poor controllability of inhalation exposure; (ii) less cytotoxicity of water-soluble CNTs than non-functionalized particles [4]; and more importantly, (iii) functionalized CNTs have shown exciting bioapplications. For example, engineered carbon nanotubes (CNTs) have been extensively utilized as cancer theranostics [1], serving as composite nanomaterials for cancer imaging [5], drug loading [6, 7], and photothermal therapy [8, 9].

All cancers arise as a result of alternations that have occurred in the DNA sequence of the genomes of cancer cells [10]. The tumor suppressor p53 gene acts as a major defense against cancer; and it is well-established that over half of all human cancers bear a p53 gene mutation [11]. Information concerning the potential hazards in p53-deficient individuals caused by CNTs exposure is still unclear, despite demonstrations in previous reports that p53-dependent responses occur with other exogenous factors such as radiation [12–14] and environmental pollutant [15]. The p53 heterozygous (p53^{+/-}) mouse model is a cancer-prone model, and was originally developed to facilitate the understanding of the role of p53 in protecting cells from exogenous factors induced DNA damage [16]. In addition, embryonic development is extremely sensitive to chemical toxins in water, food and drug formulations [17]. Here, we have chosen fetuses with different p53 genotypes as a model system of cancer-susceptible gene, derived from p53 heterozygous (p53^{+/-}) mothers that were injected with surface-modified CNTs during pregnancy, to evaluate potential differences in fetotoxic effects of the nanotubes on fetal development and growth. To investigate the biodistribution and fetotoxicity of particles, short single-walled CNTs (SWCNTs) and short multiwalled CNTs (MWCNTs) of similar surface potential and length--but with different outer diameters of <8 nm (MWCNT-8), 20–30 nm (MWCNT-20) and ~50 nm (MWCNT-50), respectively--were functionalized with PL-PEG-NH₂ by following a previously reported procedure [18], then administered to the pregnant mice.

2. Materials and Methods

2.1. Amine-functionalized single-walled and multi-walled carbon nanotubes (CNTs)

Amine-functionalized CNTs were prepared by reacting CNTs with PL-PEG-NH₂ (1, 2-distearoyl-*sn*-glycero-3-phosphoethanolamine-N-[amino(polyethylene glycol)-2000], Avanti Polar Lipids) as previously reported [5]. Briefly, 20 mg CNTs (Cheap tube Inc, VT) was added to 3-fold excess of PL-PEG-NH₂ in 5 ml distilled water. Then, the solution was dispersed for 1 h via probe sonication using a VCX-750 ultrasonic processor (Sonics & Materials, Newtown, CT). The probe was driven at 40% of the instrument's maximum amplitude in an ice-bath. After sonication, the resulting solution was purified by dialysis

membrane (MW 10000) in distilled water for 3 days by changing fresh solution every 6–12 h. Finally, the particles were collected by a centrifugal filter (3 k cutoff, Millipore) and concentrated to 5 mg mL⁻¹ in distilled water.

2.2. Cells and mice

Mouse embryonic fibroblasts (MEFs) were isolated from 13.5 to 14.5 day embryos using a standard protocol [19] and maintained in DMEM supplemented with 15% FBS. The p53^{+/-} (C57BL/6J) male and female mice were obtained from Jackson Laboratories. All mice were maintained and handled in accordance with the NIH Animal Care and Use Committee. To acquire p53^{+/-} pregnant mice, p53^{+/-} male and female mice at 8–10 weeks old were mated for one day. After 10.5 days, the pregnant mice were identified and the mice with more than 2 g of increased body weight were used for further experiments.

2.3. Fetotoxicity

Different CNTs were injected intravenously through tail vein into pregnant p53^{+/-} mice (n = 6/group) on the indicated days. The body weight of pregnant p53^{+/-} mice was measured each day. All mice were sacrificed after being anaesthetized at gestational day 17.5 (GD 17.5). The fetuses and placenta of each mouse were isolated, examined and weighed. To study the recovery effect of MWCNT-50-NAC on brain deformity, p53^{+/-} pregnant mice were treated with MWCNT-50 or MWCNT-50-NAC intravenously through tail vein on the indicated days. To study the survival rate of offspring, pregnant p53^{+/-} mice were injected with MWCNT-50 at GD 10.5, GD 12.5 and GD 15.5. After natural delivery, the survival percentage of offspring was recorded within 30 days.

2.4. Identification of p53 genotypes

Identification of p53 genotypes was performed by a p53 genotype polymerase chain reaction (PCR) protocol [20]. The primers were listed in supporting information. After running PCR, the products were examined by the agarose gel electrophoresis. The molecular weight of 620 bp and 1069 bp were identified as p53^{+/+} and p53^{-/-}, respectively. p53^{+/-} showed both bands in a gel.

2.5. Labeling of radioisotope ⁶⁴Cu and positron emission tomography (PET) imaging

The radioisotope ⁶⁴Cu (freshly made from the NIH cyclotron facility) was labeled onto CNTs by introducing a crosslinker DOTA-NHS ester (Macrocyclics Inc, Dallas, TX). Briefly, 2 mg CNTs were reacted with 0.2 mg DOTA-NHS ester in 2 ml borate buffer (pH = 9.0). The mixture was stirred at room temperature for 4 h, and subsequently, was purified by dialysis membrane (MW 3500) in distilled water. The resultant samples were concentrated into 0.5 ml distilled water with a centrifugal filter (3 k cutoff, Millipore). Then, the particles were chelated with 2 mCi ⁶⁴Cu for 1 h in NH₄Ac buffer (pH = 5.4). The resultant samples were purified and collected by a centrifugal filter. Prior to injection of ⁶⁴Cu-CNT, the coupling of labeled ⁶⁴Cu on the particles was confirmed.

Pregnant p53^{+/-} mice were injected with different types of ⁶⁴Cu-labeled CNTs via tail vein at GD 15.5. PET scans and image analysis were performed using an Inveon microPET

scanner (Siemens) at different time points post injection. The details of small animal PET imaging and the region-of-interest (ROI) analysis have been previously reported[21].

2.6. TEM analysis

At 48 h postinjection of different CNTs, mice were sacrificed under an aesthesia, and the placenta and fetal liver were fixed in 2% gluteraldehyde and 2.5% paraformaldehyde for 2 h. Small pieces of tissue collected from these samples were washed with phosphate buffer, postfixed in sodium cacodylate-buffered 1.5% osmium tetroxide for 60 min at 4 °C, dehydrated using a series of ethanol concentrations, and embedded in Epon resin. The resin was polymerized at 60 °C for 48 h. Ultrathin sections (50–70 nm) obtained with an ultramicrotome were stained with 5% aqueous uranyl acetate and 2% aqueous lead citrate and imaged under transmission electron microscope (TEM).

2.7. Nuclear DNA damage assay

DNA integrity was assessed using a Long PCR (L-PCR) assay as described previously [22]. Briefly, total DNA was extracted from MEFs or mouse liver and placenta using the DNeasy Blood & Tissue Kit (QIAGEN). A 6.5 kb mouse nuclear genome fragment was amplified using GeneAmp XL PCR kit. The primers were shown in the supporting information. Products were quantified by PicoGreen (Molecular Probes) fluorescence detection.

2.8. Western blotting of p21 and Bax expression

Antibody sources were as follows: mouse p21 (Calbiochem), Bax (Cell Signaling), and GADPH (Ambion). Briefly, protein isolated from different p53-status MEF cells were solubilized in cold lysis buffer with protease inhibitor cocktail (Roche), resolved by Tris-glycine SDS PAGE, and transferred to Immobilon-P membrane (Millipore). Standard ECL western blotting was performed (GE Healthcare).

2.9. Real-time PCR of p21 and Bax expression

RNA was isolated from mouse fetal liver and placenta tissues using the RNeasy Fibrous Tissue Mini Kit (QIAGEN) or from different p53-status MEFs by using the poly(dT) magnetic bead system (Invitrogen), reverse transcribed using Superscript II (Invitrogen), and mouse p21 and Bax gene expression were quantified by real-time PCR using SYBR green fluorescence on a 7900HT Sequence Detection System (Applied Biosystems) (RT-PCR). The primers were provided in the supporting information.

2.10. Data and statistical analysis

All graphs were constructed and statistical analysis performed using Graphpad Prism software v.5.00 (GraphPad Software). A one-way ANOVA with a post-hoc Tukey test was used to identify significant differences among treatment groups. Significance was set at $p < 0.05$ unless otherwise stated.

3. Results

3.1. Effect of functionalized CNTs on fetal development and survival

The CNT particles dispersed well in aqueous solutions (Fig. 1). The properties and purities of the particles are characterized in Tables 1 and S1. To elucidate the fetotoxicity of SWCNTs and MWCNTs on fetuses of differing p53 genetic backgrounds, p53^{+/-} pregnant mice were prepared by mating p53^{+/-} male and p53^{+/-} female mice prior to injection of particles (Scheme S1). A repeated dose was firstly used to explore whether SWCNTs and MWCNTs affect fetal development during the organogenesis period (gestational day 9.5–16.5). [23, 24] We injected the CNTs intravenously (200 μ l, 2 mg kg⁻¹) into different p53^{+/-} pregnant mice at, variously, gestational day 10.5 (GD 10.5), 12.5 (GD 12.5) or 15.5 (GD 15.5), following Timeline 1 of Scheme S2. Compared with untreated mice, the maternal body weight of mice treated with MWCNT-20 and MWCNT-50 decreased after injection ($p < 0.05$), whereas those treated with SWCNTs and MWCNT-8 did not present significant changes in weight (Fig. 2A). At GD 17.5, we euthanized the mice and isolated their fetuses to determine CNTs induced fetotoxicity. As shown in Fig. S2, no significant difference is observed with respect to the number of fetuses per litter in the untreated and CNT-treated groups, while the body weight of fetuses whose pregnant mothers had been treated with MWCNT-20 and MWCNT-50 showed $7.1 \pm 5.2\%$ ($p < 0.05$) and $23.2 \pm 7.8\%$ ($p < 0.01$) decreases over the control fetuses, respectively (Fig. 2B). It is worth noting that the MWCNT-50 group displayed “crown-shaped” tissue malformations of their brains (Fig. 2C, arrow). We found $15.1 \pm 1.1\%$ brain deformity in the MWCNT-50-treated fetuses, which was not observed in the control and other particle-treated groups. The results indicate that MWCNT-50 has more fetotoxicity than SWCNT, MWCNT-8 and MWCNT-20 at the same dose, as manifested by fetal brain deformity and restricted fetal growth.

To determine the potential long-term fetotoxicity of CNTs, MWCNT-50 (200 μ l, 2 mg kg⁻¹ or 5 mg kg⁻¹) was chosen to inject intravenously into different p53^{+/-} pregnant mice at, variously, GD 10.5, GD 12.5 and GD 15.5 (Timeline 2, Scheme S2). After natural delivery of fetuses, the fetuses were collected and the survival of offspring was recorded over 30 days. We did not find adverse effects on offspring survival for mice receiving multiple administrations of 2 mg kg⁻¹ MWCNT-50 (data not shown). However, as shown in Fig. 2D, the lethal phenomenon is not observed in untreated fetuses within 30 days ($n = 50$) when exposed to repeated doses of 5 mg kg⁻¹ MWCNT-50, whereas the survival of MWCNT-50-treated fetuses ($n = 43$) dramatically drop within the initial 5 days of post-delivery, displaying more than a 20% lethality rate of offspring. These results showed that MWCNT-50 not only induced abnormal fetal development but also affected the survival of offspring.

3.2. p53 genotype-dependent fetotoxicity of functionalized MWCNT-50

To further examine the fetotoxicity of particles on different genotypes of fetuses at different developmental stages, MWCNT-50 was injected intravenously into different p53^{+/-} pregnant mice at GD 10.5 (Timeline 3, Scheme S2) and GD 15.5 (Timeline 4, Scheme S2) in single doses (200 μ l, 5 mg kg⁻¹). Unlike the three doses repeated administration, the maternal body weight gain of mice treated with single dose MWCNT-50 at GD 10.5 or GD

15.5 was similar to the untreated group (Fig. S3). At GD 17.5, the fetuses and placentas were isolated, and subsequently the development and body weight of fetuses were evaluated. As shown in Fig. 3A and B, MWCNT-50 do not obviously change the fetal body weight with injection at GD 10.5 ($n = 34$), but more readily induced brain deformity. After determining the genotypes of fetuses, we found about $50 \pm 9.6\%$ of $p53^{-/-}$ fetuses displayed obvious brain deformity (arrow), while the malformation was not observed in the untreated and MWCNT-50-treated $p53^{+/+}$ and $p53^{+/-}$ fetuses. No obvious abnormal development of fetuses was seen at GD 15.5 injection of particles ($n = 37$), but the body weight of fetuses significantly decreased compared with the untreated fetuses (Fig. 3C and D). The average body weight of $p53^{+/+}$ fetuses was about $87.7 \pm 2.9\%$ of the untreated fetuses ($p < 0.01$). These results demonstrate that MWCNT-50 affects fetal development and growth in a $p53$ genotype-dependent manner at different developmental stages.

3.3. Imaging the biodistribution of SWCNTs and MWCNTs

Knowledge of the biodistribution and translocation of nanoparticles is a critical factor to evaluation of their *in vivo* toxicity. The blood-placenta barrier (BPB) prevents the passage of many exogenous materials between the maternal and fetal blood. It is reported, for example, that high-molecular weight drugs ($>1,000$ Da) do not penetrate the placental barrier by passive diffusion [25]. However, previous reports have shown that some nanoparticles, such as those of silica and titanium dioxide, will penetrate mouse placental tissue [17], which implies that nanoparticles might directly disrupt the blood-placenta barrier and/or are actively transported through it. Based on the fetotoxicity of CNTs, above, we hypothesized that CNTs might penetrate mouse placental tissue, and subsequently, directly affect fetal development and growth. To address the hypothesis, we explored the biodistribution patterns of SWCNT and MWCNT by labeling the nanoparticles with positron emitting radionuclide ^{64}Cu ($t_{1/2} = 12.7$ h). After intravenous injection of ^{64}Cu -labeled SWCNT, MWCNT-8, MWCNT-20 and MWCNT-50, the $p53^{+/-}$ pregnant mice ($n = 4/\text{group}$) were imaged by positron emission tomography (PET) at multiple time points up to 48 h (Fig. 4A and Fig. S4). Similar to other reported behaviors of nanoparticles, including those of CNT-based formulations, the tested SWCNT and MWCNT formulas had a tendency to accumulate in the liver. At 48 h postinjection, SWCNT, MWCNT-8, MWCNT-20 and MWCNT-50 exhibited high liver uptakes of 11.9 ± 2.3 , 10.3 ± 1.2 , 12.2 ± 0.9 and 12.1 ± 1.4 %ID/g (injected dose per gram of tissue), respectively (Fig. S5). Obvious accumulation in the uterus of the pregnant mice (white circle) was also observed.

To confirm the biodistribution of the particles in the uterus, the fetuses were isolated and imaged *ex vivo*. Fig. 4B displays the accumulation of SWCNT, MWCNT-8, MWCNT-20 and MWCNT-50 in the fetal liver and placenta. Quantification of the radioactivity found negligible difference in the fetal liver (~ 20 %ID/g) and placenta (~ 5 %ID/g) among the 4 carbon materials (SWCNT, MWCNT-8, MWCNT-20 and MWCNT-50) at 48 h postinjection (Fig. 4C). By identifying the genotypes of fetuses, we also found similar uptake of particles in fetuses of different $p53$ backgrounds (Fig. 4D). These results suggest that the accumulation of these CNTs in the fetal liver and placenta is independent of size and $p53$ -related genotypes of fetuses.

TEM analysis confirmed the distribution of SWCNTs, MWCNT-8, MWCNT-20 and MWCNT-50 in the liver and placenta of fetuses (Fig. 4E). No particles were observed in the fetal brains of mice treated with these CNTs (Fig. S6). We also observed the accumulation of particles in the liver of pregnant mice. The results were consistent with the PET imaging and confirmed the biodistribution of CNTs in the pregnant mice.

3.4. Apoptosis and cell cycle arrest by MWCNT-50

DNA damage is thought to be responsible for initiation of the abnormal development of fetuses caused by various stresses, such as numerous drugs and environmental chemicals. [26] In response to DNA damage, the induction of p53 triggers multiple cellular programs, such as cell cycle arrest and apoptosis [27, 28] that are essential for fetal development. To explore the mechanism of MWCNT-50-induced p53-related fetotoxicity, we postulated that MWCNT-50 triggers p53-dependent apoptosis and cell cycle arrest by inducing DNA damage of fetuses, which in turn causes brain deformity and the slowed weight gain of fetuses. To test this hypothesis, MWCNT-50 was injected intravenously into pregnant p53^{+/-} mice at GD 10.5 in a single dose; then at GD 17.5 the fetuses and placentas were isolated and the development and body weight of fetuses were evaluated. The experiment was then repeated with one difference: the MWCNT-50 was injected intravenously into pregnant p53^{+/-} mice at GD 15.5 in a single dose, rather than GD 10.5. In both experiments, placenta and fetal liver from each fetus were collected, total DNA was extracted and nuclear DNA (nDNA) integrity was measured as described in the Materials and Method section. The results of nDNA integrity at GD 15.5 were similar to those at GD 10.5 exposure of MWCNT-50. We found that MWCNT-50 can induce nDNA damage to all three genotypes in both fetal liver (Fig. 5A) and placenta (Fig. 5B). It should also be noted that p53^{-/-} fetuses were more vulnerable to damage caused by MWCNT-50 than the other two genotypes (p53^{+/+} and p53^{+/-}).

We next used primary cells, mouse embryonic fibroblasts (MEFs), to verify that MWCNT-50 can induce nDNA damage as shown in placenta and fetal liver *in vivo*. Different p53-related genotypes of MEFs were isolated from 13.5 to 14.5 day embryos using a standard protocol and maintained in DMEM supplemented with 15% FBS. To understand the interaction between particles and MEFs, first we verified cellular uptake of FITC-labeled MWCNT-50 (MWCNT-50-FITC) by incubating MEFs with particles (10 µg/ml) for 2 h. As shown in Fig. S7, we found that MWCNT-50-FITC was mainly distributed in the cytoplasm, and no significant difference in fluorescence intensity was present in any of the three genotypes of MEFs, indicating similar ability of the three MEFs to take up MWCNT-50-FITC. Next, we incubated MWCNT-50 (10 µg/ml) with three p53 genotyped MEFs for either 24 h or 48 h. With this treatment regime, nDNA integrities of all three cells were reduced compared to untreated cells (Fig. S8). Consistent with the *in vivo* results, p53^{-/-} MEFs showed more DNA damage than p53^{+/+} and p53^{+/-} cells after particle treatment. These results further confirmed that MWCNT-50 induces fetotoxicity through DNA damage.

In another test of whether MWCNT-50 triggers p53-dependent apoptosis and cell cycle arrest by inducing DNA damage of fetuses, we measured the expression of two p53 target

genes, Bax and p21, in the fetal liver treated with MWCNT-50 at GD 10.5 or GD 15.5, respectively. The Bax protein belongs to the multi-domain Bcl-2 family, and is an important marker of p53-mediated apoptosis [29]. p21 stimulated by p53 is essential in sustaining the G₂ arrest of cell cycle in response to DNA damage [30]. As expected, MWCNT-50 induced mRNA transcription of p21 and Bax in p53^{+/+} fetuses at both gestational days, but less so on p53^{-/-} fetuses (Fig. 5C and D). It is generally known that cell cycle arrest and apoptosis are required for neural tube closure, and defective closure of neural tube results in brain deformity [31]. The defects of induction of p21 and Bax in p53^{-/-} fetuses cause higher percentage of brain deformity compared to p53^{+/+} fetuses. It is known that disruption of genes involved in regulation cell proliferation leads to changes in animal growth [32]. As observed in p53^{+/+} fetuses, induction of p21 expression causes cell cycle arrest, which results in slowing body weight gain. To confirm the results, the effect of MWCNT-50 on p21 and Bax expression was also studied by western blotting in MEFs (Fig. 5E). Indeed, MWCNT-50 triggers p21 and Bax expression in a p53-dependent manner.

3.5. MWCNT-50-induced nuclear DNA damage and fetotoxicity

It has been widely reported that N-acetylcysteine (NAC) treatment can prevent oxidative DNA damage,[33] which in turn mediates p53-dependent molecular events [34]. To prevent fetotoxicity induced by MWCNT-50, we tested for potential effects of the antioxidant NAC on MWCNT-50-induced nDNA damage by loading MWCNT-50 with NAC. MWCNT-50 was mixed with NAC for 48 h, and was subsequently added to different p53 genotypes of MEFs. Supplementation with NAC had a dramatic effect on preventing MWCNT-50-induced nDNA damage (Fig. 6A). To substantiate the *in vitro* results, we co-injected NAC (100 mg kg⁻¹) and MWCNT-50 (5 mg kg⁻¹) into p53^{+/+} pregnant mice at GD 10.5 and collected the fetuses (n = 33) at GD17.5. As shown in Fig. 6B, an obvious decrease in brain deformity was found in the NAC treated p53^{-/-} fetuses, which implied that NAC loaded particles could be effective in preventing MWCNT-induced DNA damage and fetotoxicity.

4. Discussion

The role of diameter in the toxicity of CNTs has been considered in previous studies. Wang *et al.* reported MWCNTs with smaller diameter showed less toxicity than the larger ones toward alveolar macrophages [35]. Similarly, Yamashita *et al.* examined the biological effects of different sized MWCNTs and SWCNTs, and found a higher potency to induce DNA damage in A549 epithelial cells and inflammatory response in the lung of mice for long and thick MWCNTs than for short and thin ones while similar SWCNTs caused little response.[36] Consistent with these results, in this study, we found that functionalized MWCNTs more readily induce fetotoxicity than SWCNTs at the same doses as a result of penetration of the BPB (Fig. 2). The size effect on fetal development was also demonstrated by comparing three MWCNTs of similar length and surface charges but with different aspect ratios (Table 1). In another report, Nagai *et al.* found that thick MWCNTs (diameter ~150 nm) were less toxic, inflammogenic, and carcinogenic than the thin ones (diameter ~50 nm) [37]. It appears that besides the size effect, translocation and biodistribution can also be key factors that determine the toxicity of CNTs [17, 38]. As such, we next explored the biodistribution of SWCNTs and MWCNTs in fetuses, and found no obvious differences in

the uptake of different CNTs in fetuses (Fig. 4). In other words, the discrepancy in fetotoxicity caused by different CNTs was not due to the amount of uptake of particles in fetuses but rather the physio-chemical properties of CNTs themselves [39], such as the content of impurities, the agglomeration state, diameter of CNTs, and specific surface area. The detailed mechanism will be further explored in our future studies.

Several studies have evaluated embryonic development toxicity or teratogenicity of CNTs. For example, Pietroiusti *et al.* observed a high percentage of early miscarriages and fetal malformations in pregnant mice exposed to oxidized CNTs [40]. Fujitani *et al.* showed various types of external and skeletal malformation in MWCNT-treated group at a dose of 2–5 mg kg⁻¹ by intraperitoneal injection [41], such as tail absence, limb deformity, rib fusion and hypophalangia. In our study, brain deformity was found in the fetal brain of mice injected with CNTs at GD 10.5, while no accumulation of particles and abnormal development of brain were observed at GD 15.5 injection (Fig. 3). We believe that two reasons are accounted for such findings: (i) Direct effect of CNTs on brain deformity. The blood-brain barrier (BBB) of mouse fetus develops between GD 11 and GD 17 [42]. In addition, the first blood vessels invade the outer surface of the developing neural tube at GD 10 in mouse [43], through which CNTs could have direct effects on the development of neural tube before the BBB formation; (ii) Indirect effect by placenta. CNTs might also induce toxicity by locally interfering with placental function, since we observed placental nuclear DNA damage induced by MWCNTs injected at GD 10.5 (Fig. 5B) at which neural tube closure occurs [44].

It is now becoming clear that, in addition to its tumor suppressor role, p53 is an important teratological suppressor gene that protects the embryo from DNA damage caused by drugs and environmental chemicals [45]. It was reported that loss of p53 results in a marked increase in developmental anomalies of mice exposed to environmental insults such as carcinogens or X-irradiation [15, 46]. Furthermore, normal p53 function is essential for preventing the passage of DNA damage to the next generation of cells, by causing cell-cycle arrest or apoptosis [47, 48]. It was also shown that *in vivo* apoptosis mediated by p53 during development can eliminate mistakes by “cellular proofreading”. [49] Consistent with those studies, our experiments showed abnormal development of brain in the p53^{-/-} fetuses exposed to MWCNT-50 at GD 10.5 but not in those in the p53^{+/+} and p53^{+/-} fetuses (Fig. 3). A p53^{-/-} background apparently weakens the ability to eliminate damaged cells during development, and thus allows abnormal development of the fetus brain. Apoptosis induced by MWCNT-50 was also confirmed in p53^{+/+} fetal liver and MEFs, but significantly less so in the fetus with p53^{-/-} and p53^{+/-} status (Fig. 5C and E). Furthermore, MWCNT-50 results in cell cycle arrest of p53^{+/+} fetuses and MEFs (Fig. 5D and E). Therefore, the smaller size of p53^{+/+} fetuses compared with p53^{-/-} fetuses after treatment with MWCNT-50 at GD15.5 can be explained by slow weight gain caused by p53-dependent apoptosis and cell cycle arrest. It was worth noting that GD 10.5 and GD 15.5 are critical stages of brain development and fetal growth, respectively. Our observations suggest that MWCNT-50 induced fetotoxicity is dependent on the stage of development, p53-mediated apoptosis, and cell cycle arrest in response to DNA damage.

NAC is a precursor of intracellular cysteine and glutathione that is found naturally in the body. NAC is also regulated by the FDA as a dietary supplement, since this product is a powerful antioxidant that can neutralize oxidative free radicals which cause DNA damage and mutation [33, 50–52]. Many studies showed that NAC can help prevent and treat of cancer [53, 54] and affect the course of Parkinson's disease [55], both are DNA mutation-related diseases. It has been reported that p53 has antioxidant function, which plays an important role in preventing DNA damage, and dietary supplementation p53 knockout mice with NAC prevents spontaneous tumor frequency and increases lifespan [56]. In this study, we showed that NAC can prevent MWCNTs-induced DNA damage in p53-deficient MEFs and reduce MWCNTs-caused deformity of p53 knockout fetuses (Figure 6), which suggests that co-injection of NAC can improve overall genetic stability and minimize the teratotoxicity of CNTs and may decrease the potential risk of biomedical applications of CNTs.

The concept of personalized medicine was popularized approximately a decade ago with the hope that new technical capabilities would allow to predict health risks, track disease development and predict response to therapy. In recent years, the presence of engineered nanoparticles in various bioapplications has raised concerns about their potential risks to human health. Increased understanding of the potential relationship between a person's genome and response to nanoparticle exposure is needed to individualize risk assessment and as a prerequisite for development of nanomaterial-based personalized medicine. Until now, however, it is not known whether nanoparticles can trigger differing responses in individuals of dissimilar genetic backgrounds. In this study, we chose mouse fetuses with different p53 genetic backgrounds as a model system, to evaluate potential differences in fetotoxic effects of the nanotubes. Our findings suggest that genetic background may be a major determinant of the toxicity of nanomaterials in exposed individuals, which will be very valuable in our future design of nano-carbons for bio-analysis, early diagnosis, drug/gene delivery and therapeutics [1, 57–64].

5. Conclusion

This study demonstrates for the first time the link between fetotoxicity of functionalized CNTs and p53-related genetic background. Of the CNT materials studied, MWCNT-50 directly induced body weight changes in p53 wild type (p53^{+/+}) fetuses and brain deformities in p53 knockout (p53^{-/-}) fetuses, showing a p53 status-dependent manner of fetotoxicity (Fig. 7A). The mechanism of action appears to involve MWCNT-50 induced DNA damage of fetuses that triggered p53-dependent molecular function (Fig. 7B). Given the anatomical and structural differences between mouse and human placentas, whether the MWCNTs induced fetotoxicity observed in this study can be applied to human, remains to be explored.

Supplementary Material

Refer to Web version on PubMed Central for supplementary material.

Acknowledgments

This work was supported by the Intramural Research Program, National Institute of Biomedical Imaging and Bioengineering, National Institutes of Health. We thank Dr. Henry S. Eden for proof-reading the manuscript and Ms. Myungsun Lee for drawing the scheme.

References

1. Liu Z, Liang XJ. Nano-carbons as theranostics. *Theranostics*. 2012; 2:235–7. [PubMed: 22448193]
2. Mitchell LA, Lauer FT, Burchiel SW, McDonald JD. Mechanisms for how inhaled multiwalled carbon nanotubes suppress systemic immune function in mice. *Nat Nanotechnol*. 2009; 4:451–6. [PubMed: 19581899]
3. Ryman-Rasmussen JP, Cesta MF, Brody AR, Shipley-Phillips JK, Everitt JI, Tewksbury EW, et al. Inhaled carbon nanotubes reach the subpleural tissue in mice. *Nat Nanotechnol*. 2009; 4:747–51. [PubMed: 19893520]
4. Schipper ML, Nakayama-Ratchford N, Davis CR, Kam NW, Chu P, Liu Z, et al. A pilot toxicology study of single-walled carbon nanotubes in a small sample of mice. *Nat Nanotechnol*. 2008; 3:216–21. [PubMed: 18654506]
5. Liu Z, Cai W, He L, Nakayama N, Chen K, Sun X, et al. In vivo biodistribution and highly efficient tumour targeting of carbon nanotubes in mice. *Nat Nanotechnol*. 2007; 2:47–52. [PubMed: 18654207]
6. Liu Z, Chen K, Davis C, Sherlock S, Cao Q, Chen X, et al. Drug delivery with carbon nanotubes for in vivo cancer treatment. *Cancer Res*. 2008; 68:6652–60. [PubMed: 18701489]
7. Liu Z, Fan AC, Rakhra K, Sherlock S, Goodwin A, Chen X, et al. Supramolecular stacking of doxorubicin on carbon nanotubes for in vivo cancer therapy. *Angew Chem Int Ed Engl*. 2009; 48:7668–72. [PubMed: 19760685]
8. Moon HK, Lee SH, Choi HC. In vivo near-infrared mediated tumor destruction by photothermal effect of carbon nanotubes. *ACS Nano*. 2009; 3:3707–13. [PubMed: 19877694]
9. Burke A, Ding X, Singh R, Kraft RA, Levi-Polyachenko N, Rylander MN, et al. Long-term survival following a single treatment of kidney tumors with multiwalled carbon nanotubes and near-infrared radiation. *Proc Natl Acad Sci U S A*. 2009; 106:12897–902. [PubMed: 19620717]
10. Stratton MR, Campbell PJ, Futreal PA. The cancer genome. *Nature*. 2009; 458:719–24. [PubMed: 19360079]
11. Levine AJ, Momand J, Finlay CA. The p53 tumour suppressor gene. *Nature*. 1991; 351:453–6. [PubMed: 2046748]
12. Norimura T, Nomoto S, Katsuki M, Gondo Y, Kondo S. p53-dependent apoptosis suppresses radiation-induced teratogenesis. *Nat Med*. 1996; 2:577–80. [PubMed: 8616719]
13. Baatout S, Jacquet P, Michaux A, Buset J, Vankerkom J, Derradji H, et al. Developmental abnormalities induced by X-irradiation in p53 deficient mice. *In Vivo*. 2002; 16:215–21. [PubMed: 12182118]
14. Kubota Y, Takahashi S, Sun XZ, Sato H, Aizawa S, Yoshida K. Radiation-induced tissue abnormalities in fetal brain are related to apoptosis immediately after irradiation. *Int J Radiat Biol*. 2000; 76:649–59. [PubMed: 10866287]
15. Nicol CJ, Harrison ML, Laposa RR, Gimelshtein IL, Wells PG. A teratologic suppressor role for p53 in benzo[a]pyrene-treated transgenic p53-deficient mice. *Nat Genet*. 1995; 10:181–7. [PubMed: 7663513]
16. Green DR, Kroemer G. Cytoplasmic functions of the tumour suppressor p53. *Nature*. 2009; 458:1127–30. [PubMed: 19407794]
17. Yamashita K, Yoshioka Y, Higashisaka K, Mimura K, Morishita Y, Nozaki M, et al. Silica and titanium dioxide nanoparticles cause pregnancy complications in mice. *Nat Nanotechnol*. 2011; 6:321–8. [PubMed: 21460826]
18. Liu Z, Tabakman SM, Chen Z, Dai H. Preparation of carbon nanotube bioconjugates for biomedical applications. *Nature Protoc*. 2009; 4:1372–82. [PubMed: 19730421]

19. Parrinello S, Samper E, Krtolica A, Goldstein J, Melov S, Campisi J. Oxygen sensitivity severely limits the replicative lifespan of murine fibroblasts. *Nat Cell Biol.* 2003; 5:741–7. [PubMed: 12855956]
20. Dumble ML, Donehower LA, Lu X. Generation and characterization of p53 mutant mice. *Methods Mol Biol.* 2003; 234:29–49. [PubMed: 12824523]
21. Gao H, Kiesewetter DO, Zhang X, Huang X, Guo N, Lang L, et al. PET of glucagonlike peptide receptor upregulation after myocardial ischemia or reperfusion injury. *J Nucl Med.* 2012; 53:1960–8. [PubMed: 23139087]
22. Santos JH, Meyer JN, Mandavilli BS, Van Houten B. Quantitative PCR-based measurement of nuclear and mitochondrial DNA damage and repair in mammalian cells. *Methods Mol Biol.* 2006; 314:183–99. [PubMed: 16673882]
23. Ding H, Wu X, Kim I, Tam PP, Koh GY, Nagy A. The mouse *Pdgfc* gene: dynamic expression in embryonic tissues during organogenesis. *Mech Dev.* 2000; 96:209–13. [PubMed: 10960785]
24. Peters KG, Werner S, Chen G, Williams LT. Two FGF receptor genes are differentially expressed in epithelial and mesenchymal tissues during limb formation and organogenesis in the mouse. *Development.* 1992; 114:233–43. [PubMed: 1315677]
25. Menezes V, Malek A, Keelan JA. Nanoparticulate drug delivery in pregnancy: placental passage and fetal exposure. *Curr Pharm Biotechnol.* 2011; 12:731–42. [PubMed: 21342124]
26. Zhang XP, Liu F, Cheng Z, Wang W. Cell fate decision mediated by p53 pulses. *Proc Natl Acad Sci U S A.* 2009; 106:12245–50. [PubMed: 19617533]
27. Purvis JE, Karhohs KW, Mock C, Batchelor E, Loewer A, Lahav G. p53 dynamics control cell fate. *Science.* 2012; 336:1440–4. [PubMed: 22700930]
28. Zhang XP, Liu F, Wang W. Two-phase dynamics of p53 in the DNA damage response. *Proc Natl Acad Sci U S A.* 2011; 108:8990–5. [PubMed: 21576488]
29. Zinkel S, Gross A, Yang E. BCL2 family in DNA damage and cell cycle control. *Cell death and differentiation.* 2006; 13:1351–9. [PubMed: 16763616]
30. Mirzayans R, Andrais B, Scott A, Murray D. New insights into p53 signaling and cancer cell response to DNA damage: implications for cancer therapy. *J Biomed Biotechnol.* 2012; 2012:170325. [PubMed: 22911014]
31. Yamaguchi Y, Shinotsuka N, Nonomura K, Takemoto K, Kuida K, Yosida H, et al. Live imaging of apoptosis in a novel transgenic mouse highlights its role in neural tube closure. *J Cell Biol.* 2011; 195:1047–60. [PubMed: 22162136]
32. Ma S, Charron J, Erikson RL. Role of *Plk2* (*Snk*) in mouse development and cell proliferation. *Mol Cell Biol.* 2003; 23:6936–43. [PubMed: 12972611]
33. De Flora S, Izzotti A, D'Agostini F, Balansky RM. Mechanisms of N-acetylcysteine in the prevention of DNA damage and cancer, with special reference to smoking-related end-points. *Carcinogenesis.* 2001; 22:999–1013. [PubMed: 11408342]
34. Sablina AA, Budanov AV, Ilyinskaya GV, Agapova LS, Kravchenko JE, Chumakov PM. The antioxidant function of the p53 tumor suppressor. *Nat Med.* 2005; 11:1306–13. [PubMed: 16286925]
35. Wang X, Jia G, Wang H, Nie H, Yan L, Deng XY, et al. Diameter effects on cytotoxicity of multi-walled carbon nanotubes. *J Nanosci Nanotechnol.* 2009; 9:3025–33. [PubMed: 19452965]
36. Yamashita K, Yoshioka Y, Higashisaka K, Morishita Y, Yoshida T, Fujimura M, et al. Carbon nanotubes elicit DNA damage and inflammatory response relative to their size and shape. *Inflammation.* 2010; 33:276–80. [PubMed: 20174859]
37. Nagai H, Okazaki Y, Chew SH, Misawa N, Yamashita Y, Akatsuka S, et al. Diameter and rigidity of multiwalled carbon nanotubes are critical factors in mesothelial injury and carcinogenesis. *Proc Natl Acad Sci U S A.* 2011; 108:E1330–8. [PubMed: 22084097]
38. Choi HS, Ashitate Y, Lee JH, Kim SH, Matsui A, Insin N, et al. Rapid translocation of nanoparticles from the lung airspaces to the body. *Nat Biotechnol.* 2010; 28:1300–3. [PubMed: 21057497]
39. Sharifi S, Behzadi S, Laurent S, Forrest ML, Stroeve P, Mahmoudi M. Toxicity of nanomaterials. *Chem Soc Rev.* 2012; 41:2323–43. [PubMed: 22170510]

40. Pietroiusti A, Massimiani M, Fenoglio I, Colonna M, Valentini F, Palleschi G, et al. Low doses of pristine and oxidized single-wall carbon nanotubes affect mammalian embryonic development. *ACS Nano*. 2011; 5:4624–33. [PubMed: 21615177]
41. Fujitani T, Ohyama K, Hirose A, Nishimura T, Nakae D, Ogata A. Teratogenicity of multi-wall carbon nanotube (MWCNT) in ICR mice. *J Toxicol Sci*. 2012; 37:81–9. [PubMed: 22293413]
42. Stewart PA, Hayakawa K. Early ultrastructural changes in blood-brain barrier vessels of the rat embryo. *Brain Res Dev Brain Res*. 1994; 78:25–34.
43. Bauer HC, Bauer H, Lametschwandtner A, Amberger A, Ruiz P, Steiner M. Neovascularization and the appearance of morphological characteristics of the blood-brain barrier in the embryonic mouse central nervous system. *Brain Res Dev Brain Res*. 1993; 75:269–78.
44. Ybot-Gonzalez P, Gaston-Massuet C, Girdler G, Klingensmith J, Arkell R, Greene ND, et al. Neural plate morphogenesis during mouse neurulation is regulated by antagonism of Bmp signalling. *Development*. 2007; 134:3203–11. [PubMed: 17693602]
45. Torchinsky A, Toder V. Mechanisms of the embryo's response to embryopathic stressors: a focus on p53. *J Reprod Immunol*. 2010; 85:76–80. [PubMed: 20227113]
46. Armstrong JF, Kaufman MH, Harrison DJ, Clarke AR. High-frequency developmental abnormalities in p53-deficient mice. *Curr Biol*. 1995; 5:931–6. [PubMed: 7583151]
47. Clarke AR, Gledhill S, Hooper ML, Bird CC, Wyllie AH. p53 dependence of early apoptotic and proliferative responses within the mouse intestinal epithelium following gamma-irradiation. *Oncogene*. 1994; 9:1767–73. [PubMed: 8183575]
48. Kuerbitz SJ, Plunkett BS, Walsh WV, Kastan MB. Wild-type p53 is a cell cycle checkpoint determinant following irradiation. *Proc Natl Acad Sci U S A*. 1992; 89:7491–5. [PubMed: 1323840]
49. Brash DE. Cellular proofreading. *Nat Med*. 1996; 2:525–6. [PubMed: 8616708]
50. De Flora S, Izzotti A, D'Agostini F, Cesarone CF. Antioxidant activity and other mechanisms of thiols involved in chemoprevention of mutation and cancer. *Am J Med*. 1991; 91:122S–30S. [PubMed: 1928203]
51. Oikawa S, Yamada K, Yamashita N, Tada-Oikawa S, Kawanishi S. N-acetylcysteine, a cancer chemopreventive agent, causes oxidative damage to cellular and isolated DNA. *Carcinogenesis*. 1999; 20:1485–90. [PubMed: 10426796]
52. De Flora S, Cesarone CF, Balansky RM, Albini A, D'Agostini F, Bennicelli C, et al. Chemopreventive properties and mechanisms of N-Acetylcysteine. The experimental background. *J Cell Biochem Suppl*. 1995; 22:33–41. [PubMed: 8538208]
53. Stephenson AP, Schneider JA, Nelson BC, Atha DH, Jain A, Soliman KF, et al. Manganese-induced oxidative DNA damage in neuronal SH-SY5Y cells: attenuation of thymine base lesions by glutathione and N-acetylcysteine. *Toxicol Lett*. 2013; 218:299–307. [PubMed: 23296100]
54. Trimmer C, Sotgia F, Whitaker-Menezes D, Balliet RM, Eaton G, Martinez-Outschoorn UE, et al. Caveolin-1 and mitochondrial SOD2 (MnSOD) function as tumor suppressors in the stromal microenvironment: a new genetically tractable model for human cancer associated fibroblasts. *Cancer Biol Ther*. 2011; 11:383–94. [PubMed: 21150282]
55. Nguyen HL, Zucker S, Zarrabi K, Kadam P, Schmidt C, Cao J. Oxidative stress and prostate cancer progression are elicited by membrane-type 1 matrix metalloproteinase. *Mol Cancer Res*. 2011; 9:1305–18. [PubMed: 21849471]
56. Sablina AA, Budanov AV, Ilyinskaya GV, Agapova LS, Kravchenko JE, Chumakov PM. The antioxidant function of the p53 tumor suppressor. *Nat Med*. 2005; 11:1306–13. [PubMed: 16286925]
57. Mandal HS, Su Z, Ward A, Tang XS. Carbon nanotube thin film biosensors for sensitive and reproducible whole virus detection. *Theranostics*. 2012; 2:251–7. [PubMed: 22448194]
58. Yang M, Meng J, Cheng X, Lei J, Guo H, Zhang W, et al. Multiwalled carbon nanotubes interact with macrophages and influence tumor progression and metastasis. *Theranostics*. 2012; 2:258–70. [PubMed: 22509194]
59. Cao L, Yang ST, Wang X, Luo PG, Liu JH, Sahu S, et al. Competitive performance of carbon “quantum” dots in optical bioimaging. *Theranostics*. 2012; 2:295–301. [PubMed: 22448196]

60. Chen Z, Ma L, Liu Y, Chen C. Applications of functionalized fullerenes in tumor theranostics. *Theranostics*. 2012; 2:238–50. [PubMed: 22509193]
61. Yang ST, Luo J, Zhou Q, Wang H. Pharmacokinetics, metabolism and toxicity of carbon nanotubes for biomedical purposes. *Theranostics*. 2012; 2:271–82. [PubMed: 22509195]
62. Shen H, Zhang L, Liu M, Zhang Z. Biomedical applications of graphene. *Theranostics*. 2012; 2:283–94. [PubMed: 22448195]
63. Zhu Y, Li J, Li W, Zhang Y, Yang X, Chen N, et al. The biocompatibility of nanodiamonds and their application in drug delivery systems. *Theranostics*. 2012; 2:302–12. [PubMed: 22509196]
64. Wu L, Luderer M, Yang X, Swain C, Zhang H, Nelson K, et al. Surface passivation of carbon nanoparticles with branched macromolecules influences near infrared bioimaging. *Theranostics*. 2013; 3:677–86. [PubMed: 24019852]

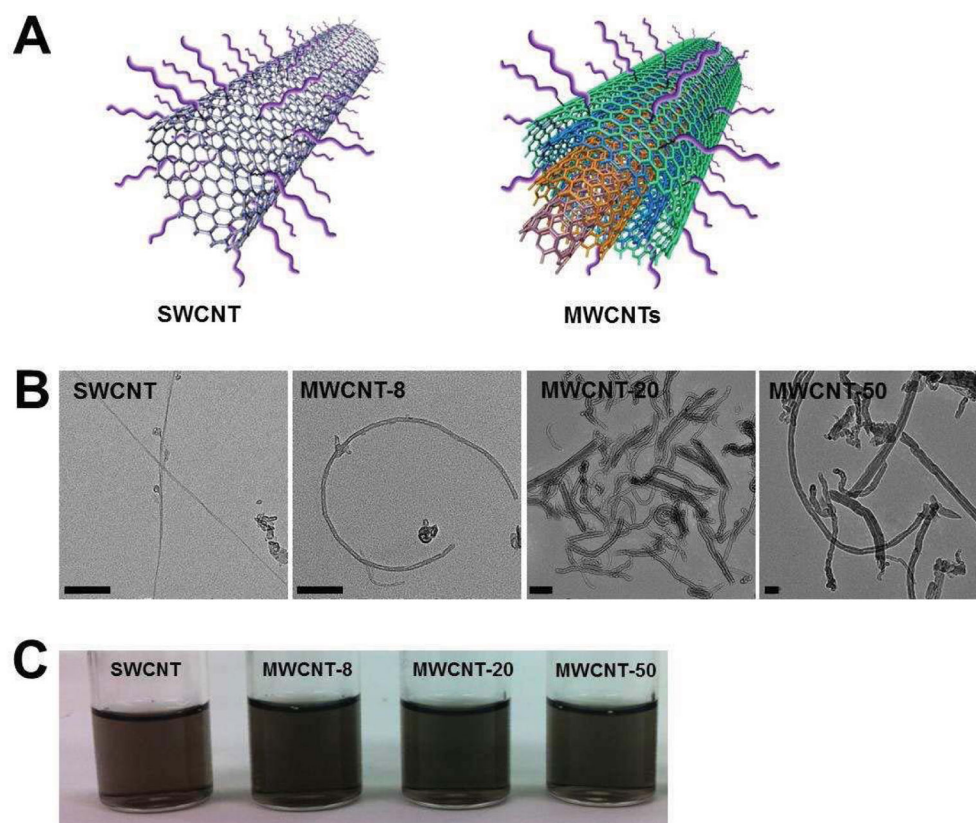


Figure 1. Preparation of water soluble CNTs by coating PL-PEG-NH₂. (A) Scheme of SWCNT and MWCNTs by coating PL-PEG-NH₂. (B) TEM images of SWCNT, MWCNT-8, MWCNT-20 and MWCNT-50. Scale bar, 50 nm. (C) SWCNT and MWCNTs showed well dispersibility in aqueous solutions.

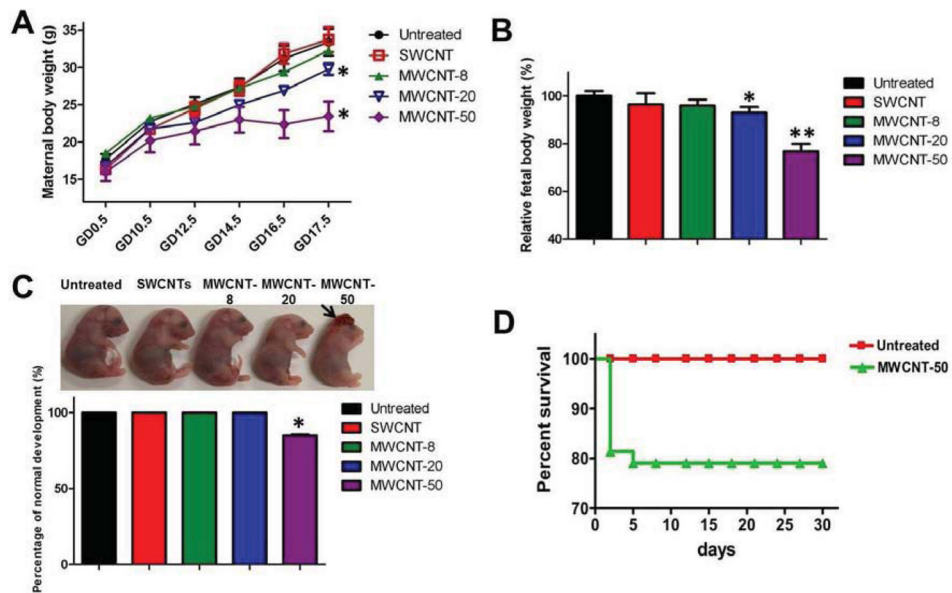


Figure 2.

CNTs induced fetotoxicity by three dose administration of different kinds of CNTs. (A) Effect of different CNTs on maternal body weight. Various kinds of CNTs were injected into $p53^{+/-}$ pregnant mice by tail vein at GD 10.5, GD 12.5 and GD 15.5. The maternal body weight was measured at different time points. At GD 17.5, the pregnant mice were euthanized and the fetuses were isolated. Values represent mean \pm s.d. (* $p < 0.05$ vs. untreated mice). (B) Changes in fetal body weight. At GD 17.5, the pregnant mice were euthanized and the fetuses were isolated, and subsequently, the body weight of fetuses was recorded (* $p < 0.05$ and ** $p < 0.01$). (C) MWCNT-50 induces brain deformity of fetal mice (arrow). Relative brain deformity of fetuses was quantified after MWCNT-50 treatment (bottom) (* $p < 0.05$). (D) MWCNT-50 affects offspring survival. MWCNT-50 was injected at GD 10.5, GD 12.5 and GD 15.5. After natural delivery of fetuses, the survival rate of offspring was observed within 30 days.

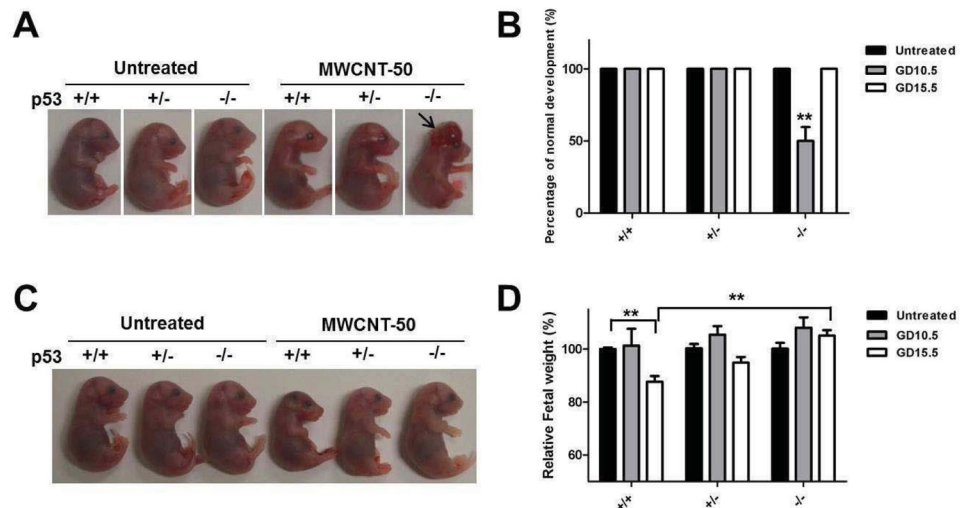


Figure 3.

MWCNT-50 induced fetotoxicity by single dose injection at GD10.5 or GD15.5. (A) Single dose of MWCNT-50 at GD 10.5 induces brain deformity in $p53^{-/-}$ mice (arrow). MWCNT-50 was injected into pregnant mice at GD 10.5 and the fetuses were isolated at GD 17.5. Statistically significant difference was found from untreated mice. (B) Relative brain deformity of fetuses was quantified after MWCNT-50 treatment at GD10.5 or GD15.5 (** $p < 0.01$). (C) Single dose of MWCNT-50 at GD 15.5 affects body weight of $p53^{+/+}$. MWCNT-50 was injected into pregnant mice at GD 15.5 and the fetuses were isolated at GD 17.5. (D) Changes in fetal body weight were evaluated of mice treated with MWCNT-50 at GD10.5 or GD15.5 (** $p < 0.01$).

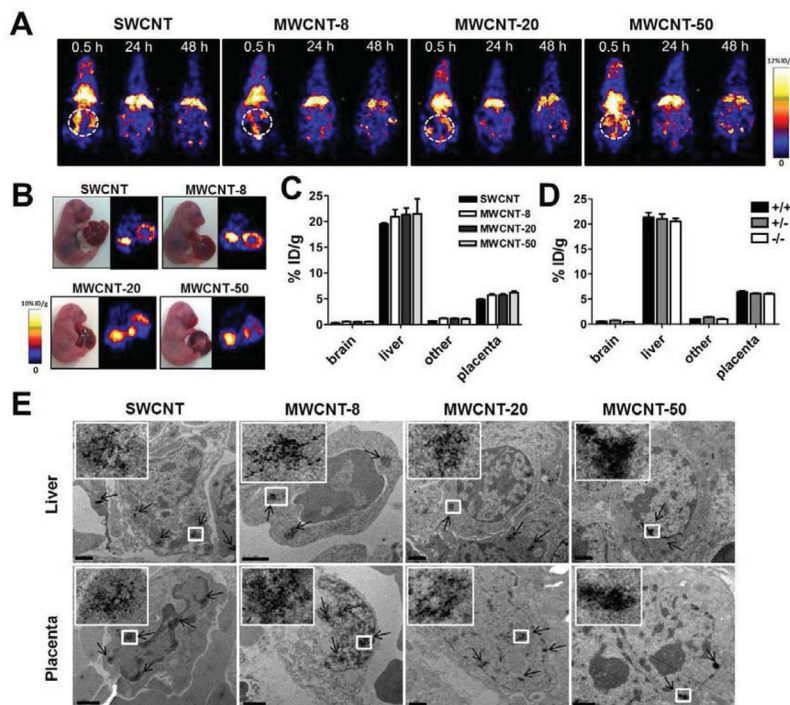


Figure 4. Positron emission tomography (PET) imaging of ^{64}Cu -labeled CNTs. (A) PET images of SWCNTs and MWCNTs in pregnant mice. CNT-DOTA- ^{64}Cu was injected into pregnant mice at GD 15.5. The images were acquired at different time points postinjection (Cycle, uterus of mice). (B) *Ex vivo* images of SWCNTs and MWCNTs in fetuses. At 48 h after injection of CNT-DOTA- ^{64}Cu , the fetuses were harvested and imaged. (C) Quantification of the biodistribution of CNTs. At 48 h after injection of CNT-DOTA- ^{64}Cu , different organs of fetuses were isolated and measured by a gamma-counter. (D) Tissue uptake analyzed in different genotypes of fetuses. (E) Liver and placenta of fetuses were observed by TEM imaging to confirm the biodistribution of CNTs (arrow). The images of CNTs are enlarged in the top left corner (Scale bar, 1 μm).

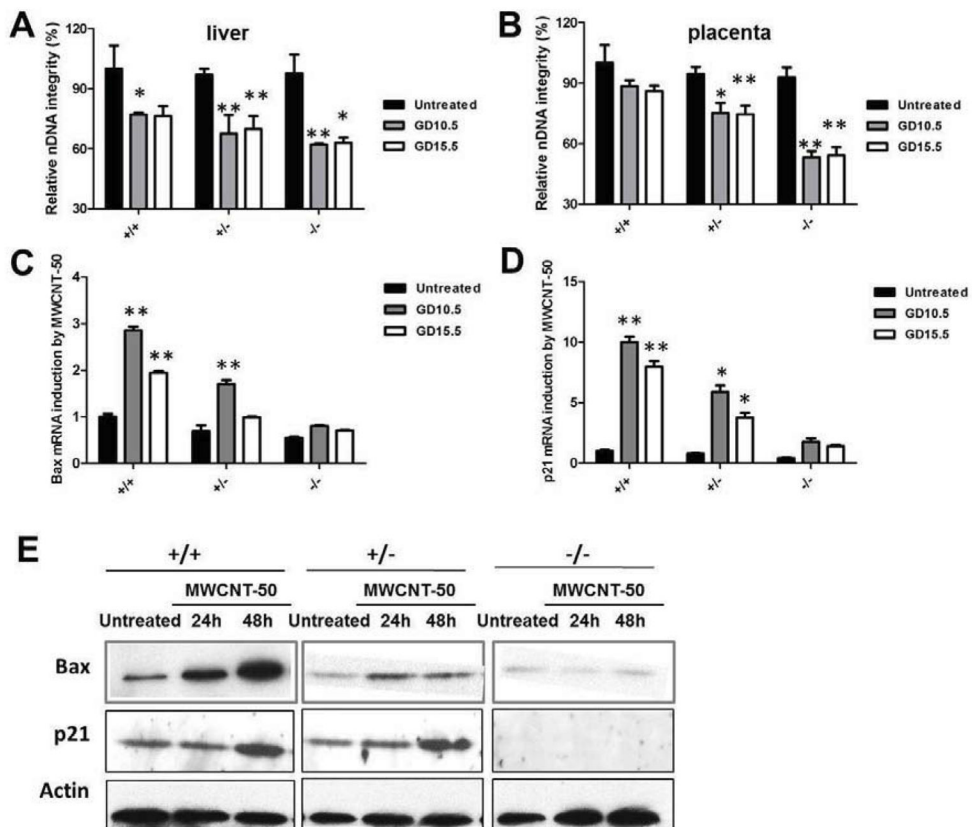


Figure 5. MWCNT-50 induces apoptosis and cell cycle arrest through DNA damage. (A, B) After treatment with MWCNT-50 at GD10.5 or GD15.5, respectively, the (A) liver and (B) placenta of fetuses were isolated. DNA of liver and placenta were subsequently extracted following analyzing nuclear DNA (nDNA) integrity (* $p < 0.05$ and ** $p < 0.01$). (C) Bax (apoptosis marker) and (D) p21 (cell cycle arrest marker) expression level were analyzed by real-time PCR (* $p < 0.05$ and ** $p < 0.01$). (E) MWCNT-50 induces apoptosis and cell cycle arrest in mouse embryonic fibroblasts (MEFs). After treatment with MWCNT-50 for 48 h, the MEFs were collected and the protein was extracted. The Bax and p21 expression levels were determined by Western blotting.

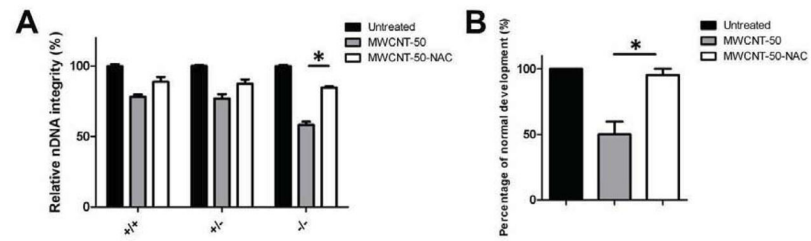


Figure 6.

NAC loading prevents MWCNT-50-induced fetotoxicity. (A) After treatment with MWCNT-50 with and without NAC for 48 h, the MEFs were collected and the DNA was extracted. Nuclear DNA integrity was analyzed. (B) Brain deformity induced by a single dose of MWCNT-50 and MWCNT-50-NAC at GD 10.5 in $p53^{-/-}$ fetuses harvested at GD 17.5 (* $p < 0.05$).

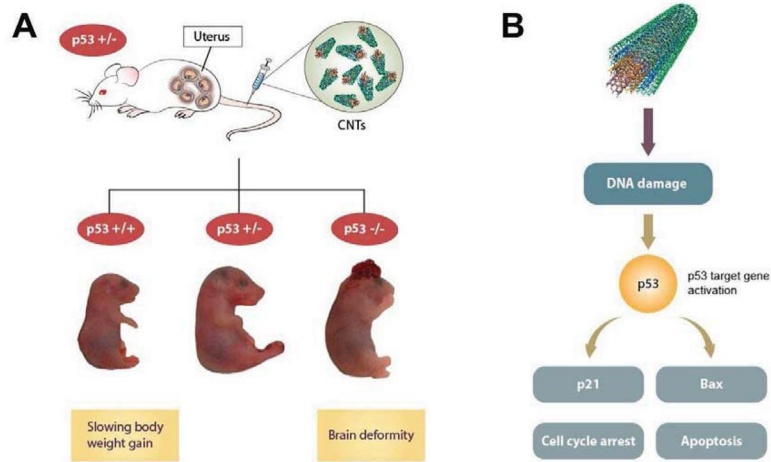


Figure 7. Schematic illustration of CNTs induced fetotoxicity. (A) Intravenous injections of functionalized CNTs into pregnant mice can induce p53-status-dependent responses in fetal development. (B) MWCNTs induced fetotoxicity by directly triggering p53-dependent apoptosis and cell cycle arrest in response to DNA damage.

Table 1

Characterization of SWCNT and MWCNTs

	Outer Diameter	Inner diameter	Zeta potential (mV in serum)	Length	Purity	Ash
SWCNT	1-2 nm	0.8-1.6 nm	-1.3±1.4	0.5-2 μm	> 90 wt%	< 1.5 wt%
MWCNT-8	<8 nm	2-5 nm	-1±1.4	0.5-2 μm	> 95 wt%	< 1.5 wt%
MWCNT-20	20-30 nm	5-10 nm	-1.9±2.1	0.5-2 μm	> 95 wt%	< 1.5 wt%
MWCNT-50	~ 50 nm	5-10 nm	-1.5±1.8	0.5-2 μm	> 95 wt%	< 1.5 wt%